



Preparation and characterization of RuCl₃ – Diamine group functionalized polymer

D. Duraczynska^{a,*}, A. Drelinkiewicz^a, E.M. Serwicka^a, D. Rutkowska-Zbik^a, E. Bielańska^a, R. Socha^a,
A. Bukowska^b, W. Bukowski^b

^a Institute of Catalysis and Surface Chemistry, Polish Academy of Sciences, 30-239 Kraków, Niezapominajek 8, Poland

^b Faculty of Chemistry, Rzeszów University of Technology, 35-959 Rzeszów, ul. W. Pola 2, Poland

ARTICLE INFO

Article history:

Received 21 December 2009

Received in revised form 9 March 2010

Accepted 13 March 2010

Available online 18 March 2010

Keywords:

Functional polymer

Ruthenium

Hydrogenation

Acetophenone

ABSTRACT

Gel-type resin with diamine functional groups, FCN, was used as a matrix for immobilization of ruthenium complexes. By reacting of RuCl₃ with swollen matrix of FCN polymer a series of Ru/FCN composites with various Ru loading (1%, 2%, and 4%) was prepared. All the characterization techniques (FT-IR, XRD, SEM, EDS, STEM, XPS, and DSC) proved the participation of functional groups in the coordination of Ru(III). These complexes contained both Cl- and N-ligands in various proportions depending on ruthenium loading in polymer. Taking into account the chelating character of N-ligands a hypothetical structure of octahedral Ru(III) complex coordinated to FCN polymer was proposed. 2%Ru/FCN when reduced by NaBH₄ exhibited catalytic activity in liquid phase hydrogenation of acetophenone. Higher selectivity in the presence of FCN supported Ru as compared to 2%Ru/Al₂O₃ catalyst toward 1-phenylethanol was observed.

© 2010 Elsevier Ltd. All rights reserved.

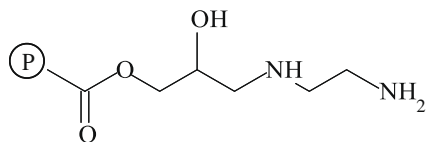
1. Introduction

Polymer supported noble metals composites have been used in a wide range of organic synthetic applications and in heterogeneous catalysis [1]. Very prominent and promising catalytic performance of Pd, Pt, Rh-polymer composites was observed in hydrogenation of cyclohexene [2], nitroaromatics [3,4] unsaturated aldehydes and alcohols [5–7], hydrosilylation of alkenes [8]. Among many conventional carriers such as Al₂O₃, TiO₂, SiO₂, C, and zeolites, polymeric supports offer unique features as potential carriers. Their hydrophobic/hydrophilic character, the presence of various functional groups and high ability to stabilize finely dispersed metal nanoparticles make polymers very attractive as potential supporting materials [9,10]. As a result of such specific properties, catalytic centers formed in polymer matrix act in the environment which essentially differs from that of conventional inorganic carriers supported noble metal catalysts [10,11]. Literature data as well as the recent results reported by Drelinkiewicz et al. [12–16] showed that the presence of polymer matrix exhibited profound role in the activity of Pt, Pd-polymer supported catalysts via an influence of polymer framework on the access of reagents to the active centers surrounded by polymer chains. In addition, functional groups of polymer may modify adsorption properties of catalytically active centers via electron interactions, especially in the case of finely dispersed metal nano-clusters. It

has been observed that specific environment of catalytically active centers located in the functionalized polymer matrices could influence not only the activity but also the selectivity of catalyzed reaction [1,17]. In contrast to the widely studied polymer supported palladium and platinum catalysts, investigation of catalytic application of less expensive Ru/polymer systems is rather limited. Recently, Sanchez-Delago et al. [18] demonstrated that Ru immobilized on poly(4-vinylpyridine) was found to be an efficient catalyst for selective hydrogenation of aromatic ring of quinoline to give 1,2,3,4-tetrahydroquinoline at 30–40 bar H₂ and ca. 100 °C. This catalyst (10 wt.% Ru) was prepared by NaBH₄ reduction of RuCl₃·xH₂O in methanol in the presence of the polymer [18]. Another study showed that Ru catalysts supported on highly hydrophilic support, i.e. potassium methacryloyl ethylene sulphate resin were efficient in partial hydrogenation of benzene to cyclohexene [19]. Interestingly, they exhibited better selectivity than Ru/C catalyst. Other Ru catalysts, obtained by reacting of RuCl₃ with chloromethylated styrene-divinyl benzene co-polymer functionalized by glycine, were found to be effective in the hydrogenation of nitrobenzene [20].

It has been shown that polymer framework, and, in particular, functional groups, played a key role in anchoring of Pt and/or Pd-ions, by facilitating formation of various coordination species acting as precursors of catalytically active centers [1]. In view of this, understanding the relation between the nature of the polymer and its bonding mode to noble metal ions is of paramount importance. This issue constitutes the main goal of present work, in which novel catalysts consisting of ruthenium complexes supported on

* Corresponding author. Tel.: +48 12 6395142; fax: +48 12 4251923.
E-mail address: ncduracz@cyf-kr.edu.pl (D. Duraczynska).



Scheme 1. The structure of FCN resin.

functionalized gel-type resin (FCN), shown in Scheme 1, were designed and prepared. In the earlier study performed by Drelinkiewicz et al. [14] this polymer served as support immobilizing coordinatively bonded palladium species. The successful application of Pd/FCN catalyst in the hydrogenation of phenylacetylene and 2-butyne-1,4-diol prompted us to apply FCN resin as potential supporting matrix for ruthenium.

In order to elucidate the nature of interactions between the functional groups of FCN polymer, e.g. C=O, NH, NH₂ (see Scheme 1) and RuCl₃ during the incorporation of ruthenium into the FCN polymer, a series of Ru/FCN composites with various content of ruthenium (1 wt.%, 2 wt.%, and 4 wt.%) were prepared and characterized by FT-IR, XRD, SEM, STEM, EDS, XPS, and DSC techniques. Catalytic properties of 2%Ru/FCN composite were evaluated in hydrogenation of acetophenone. This reaction was chosen as a model reaction because ruthenium catalysts are known to be highly selective in hydrogenation of carbonyl group in the vicinity of isolated, conjugated and aromatic double bonds [21–24].

2. Experimental

2.1. Materials

Acetophenone, and RuCl₃·xH₂O were purchased from Sigma–Aldrich while 1-phenylethanol, 1-cyclohexylethanol, cyclohexyl methyl ketone were manufactured by Fluka.

2.2. Preparation of Ru/FCN composites

The preparation route of FCN resin is based on a two-step process involving preparation of GMA-co-polymer and its functionalization by ethylene diamine. The details concerning the synthesis and characterization of FCN resin were published before [14].

The first step consisted of the synthesis of GMA co-polymer by suspension polymerization of the mixture of glycidyl methacrylate (GMA, 20 mol%), styrene (77 mol%) and diethylene glycol dimethacrylate (DEGDMA, 3 mol%). The GMA co-polymer was obtained in the form of microbeads. In the second step microbeads of GMA-co-polymer were functionalized by ethylene diamine to produce final FCN resin (Scheme 1). Functionalization was performed with 5-fold excess of ethylene diamine in DMF medium (24 h, at 80 °C). The final FCN polymer was carefully washed with DMF, methanol and methylene chloride and then dried in vacuum oven at 40 °C. The FCN resin (3% crosslinking degree) used in present work was in the form of beads 50–150 μm in size, the content of N was determined to be 2.78 wt.% [14]. THF, in which the FCN polymer swells very well, was used as a solvent medium during the preparation of Ru-composites.

Ru/FCN composites, with ruthenium loadings of 1, 2, and 4 wt.%, were synthesized as follows. Prior to incorporation of ruthenium, ca. 2 g of FCN resin was allowed to swell for 30 min in 25 ml of THF solvent. Then 15 ml of RuCl₃ aqueous solution (0.015 mol/dm³, 0.03 mol/dm³, and 0.06 mol/dm³ for 1%, 2% and 4%Ru, respectively) were added and the suspension of polymer beads in THF/aqueous medium was gently shaken until the complete discoloration of initially black solutions. The resulting dark brown or black polymer beads were separated by filtration, washed with acetone

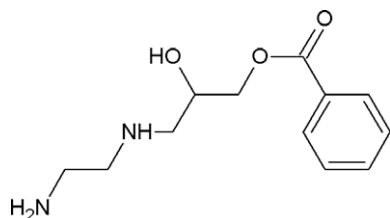
several times and dried in air. Then 10-fold excess of NaBH₄ solution in THF:CH₃OH (9:1 volume ratio) with respect to Ru was added and the catalysts were gently stirred till the evolving of gas bubbles was no longer observed. The resulting black Ru-polymer beads were filtered, washed several times with acetone and dried in air.

2.3. Preparation of Ru/Al₂O₃ catalyst

Ruthenium was incorporated into γ-Al₂O₃ carrier (BET surface area 155 m²/g, particles ca. 100 μm in size) by means of impregnation method. Prior to ruthenium incorporation, Al₂O₃ support was dried overnight in the oven at 150 °C. Then RuCl₃ aqueous solution (0.06 mol/dm³) was added (38 cm³ to 10 g of dried and cooled Al₂O₃) and the obtained mixture was vigorously stirred on water bath (~90 °C) until evaporation to dryness. The resulting black solid was dried overnight at 150 °C. Reduction was performed using 10-fold excess of NaBH₄ solution in THF:CH₃OH (9:1 volume ratio). When the evolving of gas bubbles was no longer observed, the black solid was filtered, washed several times with acetone and dried in air.

2.4. Characterization methods

The catalysts were characterized by FT-IR, XRD, SEM, EDS, STEM, XPS and DSC techniques. FT-IR studies were carried out using a Bruker–Equinox 55 spectrometer and a standard KBr pellet technique. X-ray diffraction patterns were collected on a PANalytical X'Pert Pro diffractometer using Cu Kα radiation. Morphology of Ru/FCN composites was investigated by means of Field Emission Scanning Electron Microscope JEOL JSM – 7500 F equipped with the X-ray energy dispersive (EDS) system. Two detectors were used and the images were recorded in two modes. The secondary electron detector provided SEI images and back scattered electron detector provided BSE (COMPO) micrographs. K575X Turbo Sputter Coater was used for coating the specimens with chromium (deposited film thickness – 20 nm). Energy dispersive X-ray (EDS) measurements were performed for both Ru and Cl elements. Transmission electron microscopic studies were performed with FEI Tecnai G² transmission electron microscope at 200 kV equipped with EDAX EDX and HAADF/STEM detectors. The X-ray Photoelectron Spectroscopy measurements were performed in the ultrahigh vacuum (2 × 10⁻⁷ Pa) system equipped with hemispherical analyzer (SES R4000, GammaData Scienta). The unmonochromatized Mg Kα X-ray source of incident energy of 1253.6 eV was applied to generate core excitation. The spectrometer was calibrated according to ISO 15,472:2001. The energy resolution of the system in all experiments, measured as a full width at half maximum (FWHM) for Ag 3d_{5/2} excitation line, was 0.9 eV. The spectra were calibrated for C 1s excitation at binding energy of 285.0 eV. The spectra were analyzed and processed with the use of CasaXPS 2.3.10. software. The background was approximated by Shirley algorithm and the detailed spectra were fitted with Voigt function. The accuracy of the XPS analysis is approximately 3%. DSC measurements were performed using Toledo 822 calorimeter with Star System software. The samples were heated from 30 °C to 300 °C and then cooled to 30 °C. The procedure was repeated twice. The rates of heating and cooling were adjusted to 10 °C/min. Swelling ability of pure resin, as-prepared and NaBH₄ treated Ru/FCN composites was evaluated by the measurements of bulk expanded volume in THF solvent. About 0.06 g of dry sample was placed into 1 cm³ graduated syringe and its volume was measured (V₀). Then, an excess of THF was added. Swelling equilibrium was achieved after 30 min, and the volume of expanded samples (V_s) was determined. As the measure of swelling ability the ratio V_s/V₀ was assumed. In order to predict the geometry and electronic structure



Scheme 2. Hydrocarbon chain used as a model of polymer for theoretical studies.

of possible ruthenium–polymer species, theoretical studies were done within density functional theory (DFT) with Becke–Perdew functional [25,26], as implemented in Turbomole v. 5.9.0. [27]. The resolution of identity (RI) approach [28] was applied for computing the electronic Coulomb interactions. For geometry optimizations, all electron basis sets of SVP quality were employed for all atoms (C, H, O and N) except for ruthenium, for which equivalent effective core potential was used [29]. The polymer was modeled by hydrocarbon chain carrying all functional groups (see Scheme 2), and the polymer chain was approximated by phenyl ring. It was assumed that octahedral sphere was preserved and each ruthenium atom was coordinated to the polymer chain by nitrogen atoms, and two chlorine ions completed octahedral structure.

2.5. Hydrogenation experiments

Hydrogenation experiments were carried out in an agitated batch glass reactor at constant atmospheric pressure of hydrogen and temperature 40 °C. 10 cm³ of H₂O and 10 cm³ of ACT solution in isooctane (137·10⁻⁵ mol/dm³) as well as 0.2 g of catalyst were placed in the reactor. Before the hydrogenation experiment the catalyst wetted with water was activated inside the reactor by passing gaseous hydrogen through the reactor for 45 min at 20 °C and 45 min at the temperature of reaction (40 °C in the typical procedure). The progress of reaction was monitored by gas chromatography. Samples of liquids were withdrawn from the reactor via a sampling tube at regular intervals of time and analyzed by GC method. A gas chromatograph (Clarus 500, Perkin Elmer) with He as carrier gas (flow rate 1 cm³/min) equipped with a capillary column Elite 5MS (30 m × 0.25 mm × 0.25 μm) and a flame ionization detector (FID) was used to analyze the composition of reaction mixture. The contents of acetophenone (ACT), 1-phenylethanol (PE), cyclohexyl methyl ketone (CMK), and 1-cyclohexylethanol (CE), and ethylbenzene (EB) were determined by the comparison with calibration curves.

3. Results and discussion

3.1. FT-IR spectroscopy

Fourier transform IR spectra of the parent FCN resin and Ru/FCN composites with 1%Ru and 4%Ru are shown in Figs. 1 and 2, respectively. In the FT-IR spectrum of parent FCN polymer a set of bands originating from the presence of styrene as well as carbonyl and amine functional groups can be seen [14]. Strong and broad bands located at 1714 cm⁻¹ and 1601 cm⁻¹ are ascribed to C–O stretching vibrations in the carbonyl group. The bands located within the range 1550–1655 cm⁻¹ are assigned to the N–H bonds in –NH and –NH₂ functional groups and the band 1380 cm⁻¹ to the vibrations of C–N bond [14]. In the spectral region characteristic of hydrogen bond vibrations a broad maximum located at 3430 cm⁻¹ appears (spectrum not shown).

The most noticeable spectral changes caused by the incorporation of ruthenium species are observed within the range character-

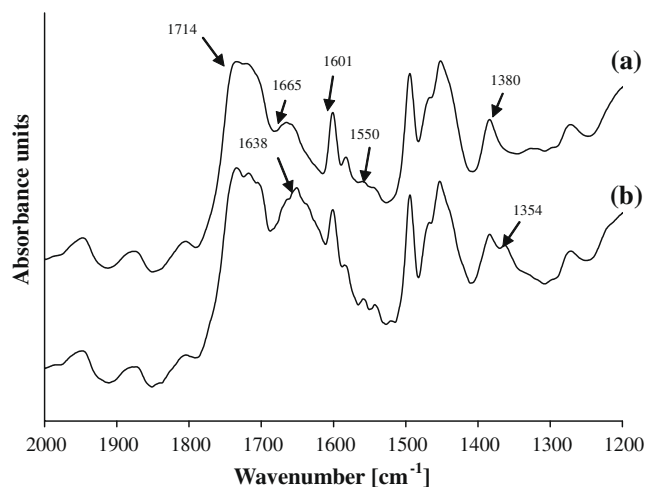


Fig. 1. FT-IR spectra of (a) FCN resin and (b) as-prepared 1%Ru/FCN.

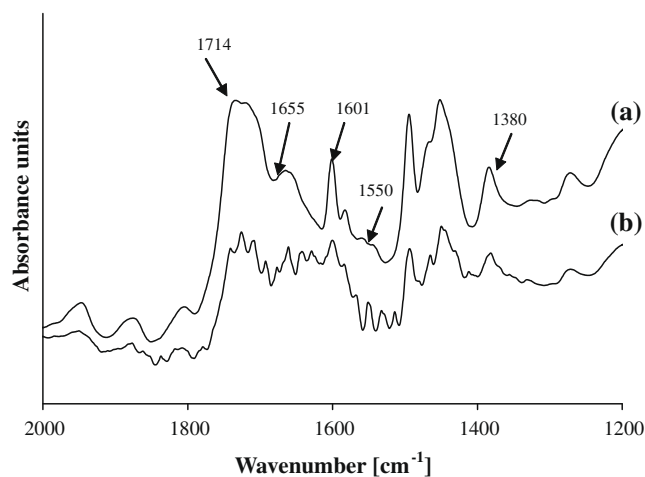


Fig. 2. FT-IR spectra of (a) FCN resin and (b) as-prepared 4%Ru/FCN.

istic of FCN functional groups. A broad new band located at ca. 1354 cm⁻¹ can clearly be seen next to the band of C–N vibration at 1380 cm⁻¹ visible in the spectra of as-received 1%Ru/FCN and 4%Ru/FCN composites (Figs. 1 and 2). In the range of N–H vibrations a new band around 1638 cm⁻¹ appears. As shown in Figs. 1 and 2, such spectral changes are observed irrespective of the loading of ruthenium in the FCN polymer. From such spectral changes it can be concluded that functional groups of FCN polymer, particularly N-groups, like –NH and –NH₂ participate in bonding of ruthenium species to polymer matrix. A similar observation has been reported by Patel et al. [20] for glycine modified chloromethylated polymer.

3.2. XRD diffraction studies

Fig. 3 shows the XRD diffraction patterns of the parent FCN polymer, as-prepared and NaBH₄ treated Ru/FCN composites. In the diffraction pattern of parent FCN polymer two broad peaks located within the 2θ region of 10–18° can clearly be seen indicating partly crystalline nature of the polymer. Incorporation of RuCl₃ results in a broadening of these reflections, particularly obvious for the peak around 11°. Such modification of the XRD pattern suggests some degree of “disordering” in polymer backbone due to incorporation of Ru-species. The effect is maintained after treat-

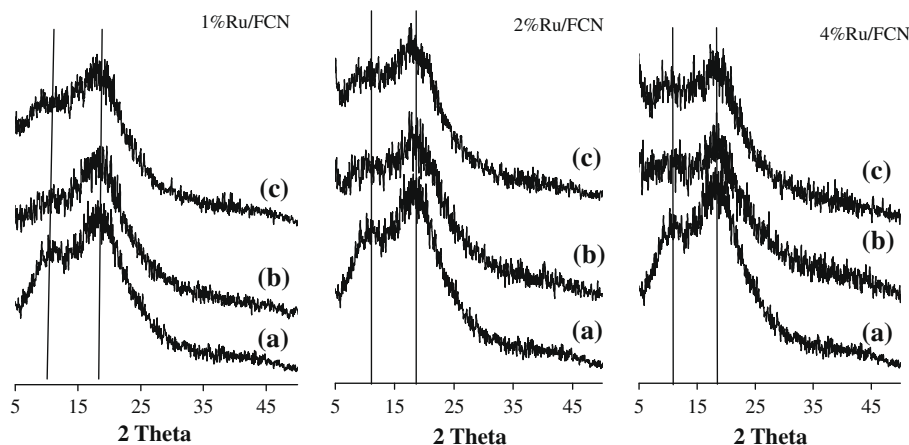


Fig. 3. XRD profiles of parent FCN resin (a), as-prepared (b) and NaBH_4 treated Ru/FCN composites (c).

ment of Ru-composites by reducing agent, NaBH_4 . Furthermore, the XRD patterns of reduced composites show no trace of peaks at $2\theta = 38.1^\circ$, 42.1° , and 44.0° characteristic of most intense reflections of crystalline Ru metal [30–32] which confirms fine dispersion of metallic Ru centers.

3.3. Electron microscopic studies (SEM, EDS)

The morphology of parent FCN polymer, as-prepared and NaBH_4 treated Ru/FCN composites was studied by scanning electron microscopy technique (SEM). Energy dispersive X-ray spectroscopy (EDS) was used to evidence the presence of Ru and Cl elements. X-ray microprobe analysis for Ru and Cl elements was performed in various grains of Ru-composites as well as in several surface areas of composite beads.

In Fig. 4a showing parent FCN, spherical beads of polymer with smooth surface can clearly be seen. Fig. 4b shows the SEM image of as-prepared 4%Ru/FCN composites. Strong changes in morphology of polymer beads are observed as a result of incorporation of RuCl_3 . The surface of Ru-containing polymer beads features highly folded texture. These folds characterize various depths and shapes and creates complex “mosaic” texture of Ru-containing spherical polymer beads (Fig. 4c). These morphological changes – folds – are very distinct and are formed in most of polymer beads. It should be noted that no such effects are observed in polymer support subjected to treatment with impregnating solution without Ru salt. This type of morphological changes was observed irrespective of the Ru loading in the polymer. At low loading of Ru in polymer (1%Ru/FCN) only few polymer beads exhibited folded morphology. As the loading of Ru is increased, the number of beads with “mosaic” texture increased. Moreover, the Ru-polymer beads differed with respect to the extent of foldings. In order to clarify the nature of such strong morphological changes, X-ray analysis was carried out for Ru and Cl elements for few beads of 4%Ru/FCN differing in the degree of folding (Fig. 5). From the data of EDS analysis of Cl/Ru atomic ratio (at./at.%) was calculated and the obtained data are collected in Table 1.

First of all, it is evident that both elements Ru and Cl are present in all polymer beads. Moreover, the values of Cl/Ru atomic ratio for smoother beads (spectra 1 and 2, Fig. 5) were 2.05 and 2.16 being only slightly smaller than that of stoichiometric Cl/Ru ratio equal to three (see Table 1). The values of Cl/Ru were lower (1.38 and 1.12) for the beads with more folded texture (spectra 7, 8 in Fig. 5). For the highly folded beads (spectra 3–6 in Fig. 5) the lowest Cl/Ru atomic ratios, below one, were observed. It can be therefore concluded that the observed strong changes in morphology of

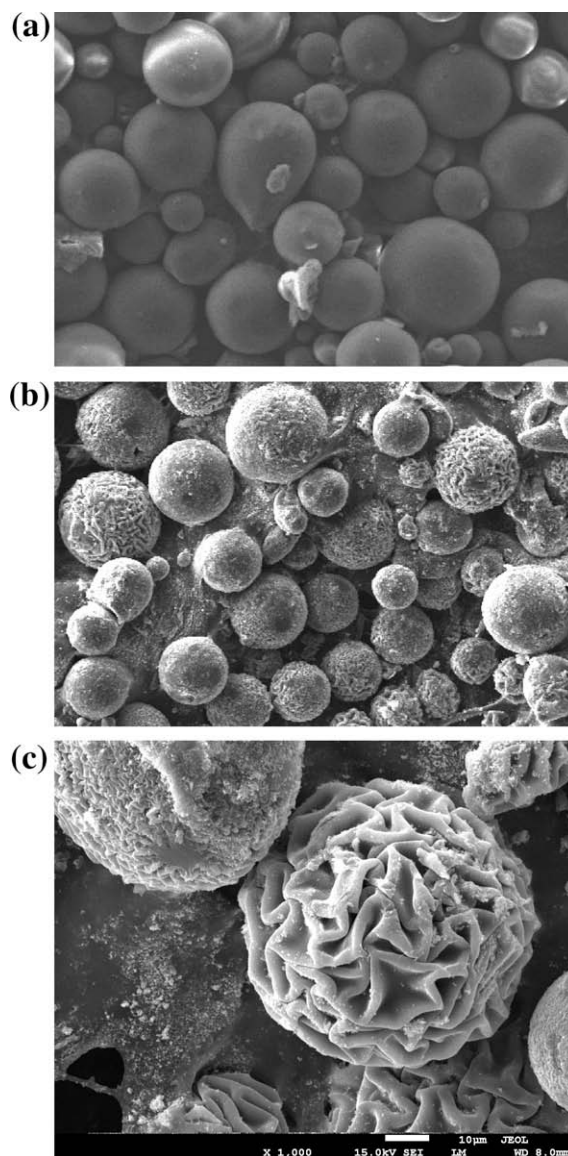


Fig. 4. SEM micrographs of (a) parent FCN ($\times 100$), (b) as-prepared 4%Ru/FCN ($\times 100$), and (c) as-prepared 4%Ru/FCN ($\times 1000$).

polymer beads are the result of Ru-species insertion. For all analyzed beads of as-prepared Ru/FCN composites the Cl/Ru atomic ra-

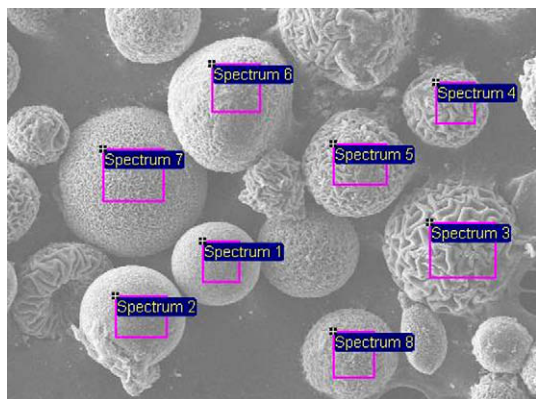


Fig. 5. SEM micrograph of as prepared 4%Ru/FCN composite with marked areas where EDS analysis was performed.

Table 1
EDS analysis of as-prepared 4%Ru/FCN.

Spectrum	Ru (at.%)	Cl (at.%)	Cl/Ru
Spectrum 1	32.75	67.25	2.05
Spectrum 2	31.68	68.32	2.16
Spectrum 3	54.61	45.39	0.83
Spectrum 4	52.27	47.73	0.91
Spectrum 5	51.96	48.04	0.92
Spectrum 6	56.38	43.62	0.77
Spectrum 7	41.98	58.02	1.38
Spectrum 8	47.08	52.92	1.12

tios were distinctly lower as compared to the stoichiometric value of RuCl_3 ($\text{Cl}/\text{Ru} = 3$). This suggests that upon the treatment of FCN polymer with RuCl_3 , the breakage of the Ru–Cl bond occurred and some of Cl–ligands were substituted by the N/O ligands from the FCN polymer (Scheme 1). The lower Cl/Ru atomic ratios observed for the most folded beads may suggest higher degree of Cl exchange by N/O ligands from the polymer. Thus, the larger participation of the functional groups of FCN polymer in the bonding to Ru-species, the more distinct morphological changes are.

Although the contents of Ru and Cl differed for individual beads of Ru-composites, the average value of Cl/Ru ratios were calculated for particular Ru/FCN composites (with 1, 2, and 4 wt.%) and they are presented in Table 2. It can be seen that as the Ru loading increases from 1% up to 4%, the Cl/Ru atomic ratio gradually increases from 0.6 to 1.12. Hence, at lower loading of Ru, functional groups of polymer are more involved in the coordination of Ru-species, and as the loading of Ru grows the participation of polymer in coordination of ruthenium gradually decreases. It should be stressed that remarkable morphological changes were also noticed upon treatment of bidentate N, O-donor sites-containing polymer (poly(S-DVB) with RuCl_3 solution [33]. Some changes in the morphology of polymer and its texture were also noticed

Table 2
The average values of EDS data for as-prepared and NaBH_4 treated Ru/FCN composites.

Sample	Ru (at.%)	Cl (at.%)	Cl/Ru
As-prepared 1%Ru/FCN	57	43	0.60
NaBH_4 treated	92.87	7.13	0.08
As-prepared 2%Ru/FCN	60.26	39.74	0.66
NaBH_4 treated	85.53	14.47	0.17
As-prepared 4%Ru/FCN	46.09	53.91	1.17
NaBH_4 treated	86.72	13.28	0.15

after the chelation of Ru(III) by N,O-ligands [20] in glycine functionalized styrene–DVB. After the treatment of Ru/FCN composites with NaBH_4 , the content of Cl strongly decreased with consequent decreasing of Cl/Ru ratio (Table 2). In reduced composites only traces of Cl are detected by the EDS analysis. The observed decrease of Cl content indicates the breakage of the Ru–Cl bonds and the subsequent removal of Cl ions upon the treatment with reducing agent. The representative SEM images of NaBH_4 treated 4%Ru/FCN composite is shown in Fig. 6. It can be seen that after the treatment of Ru/FCN sample with NaBH_4 , the complex “mosaic” texture is still preserved. However, the new irregular “bright” spots of various shapes and sizes randomly oriented and distributed throughout the polymer beads appeared. The representative SEM images of a typical “bright” spots registered at high magnification using both SEI and BSE (COMPO) detection modes are shown in Fig. 7a and b, respectively. For the comparison, typical surface morphology of untreated FCN polymer is shown in Fig. 8. A number of small spherical polymer beads – particles of very uniform sizes ($0.1 \mu\text{m}$) forming granular morphology composed of relatively regular “chains” can be seen on the surface of untreated FCN polymer. The SEI image of NaBH_4 treated 2%Ru/FCN composite shows the same type of granular morphology, however some of small polymer particles differ from the others. They are observed in the BSE images (COMPO) as the “bright” spherical particles, i.e. the polymer small spherical particles consisting of ruthenium (Fig. 7). EDS analysis carried out in areas of these “bright spots” showed predominant presence of Ru (94.4–96%) with only traces of Cl (4–6%). Thus, these bright, irregularly shaped spots observed in the BSE (COMPO) images present the particles of polymer enriched by metallic ruthenium. Fig. 9a presents STEM micrograph of NaBH_4 treated 2%Ru/FCN. At this high magnification, “bright” areas are visible throughout the whole examined sample. It is interesting to note that no separate Ru-particles were visible and no diffraction of crystalline ruthenium was observed (Fig. 9b). No crystalline ruthenium was also observed by the XRD diffraction pattern shown in Fig. 3. Thus, most likely colloidal ruthenium or nano-clusters of ruthenium were formed.

3.4. X-ray photoelectron spectroscopy

XPS measurements were employed to confirm the coordination of ruthenium by functional groups of FCN polymer. As pointed out in the literature there are relatively few reliable reference values of the photoelectron binding energy for ruthenium compounds [34–36]. Moreover, the value of BE is very sensitive to changes in the nearest environment of the Ru atom, e.g. types of ligands.

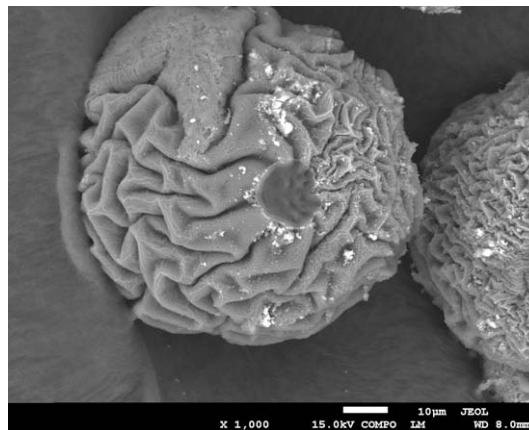


Fig. 6. SEM micrograph of NaBH_4 treated 4%Ru/FCN composites.

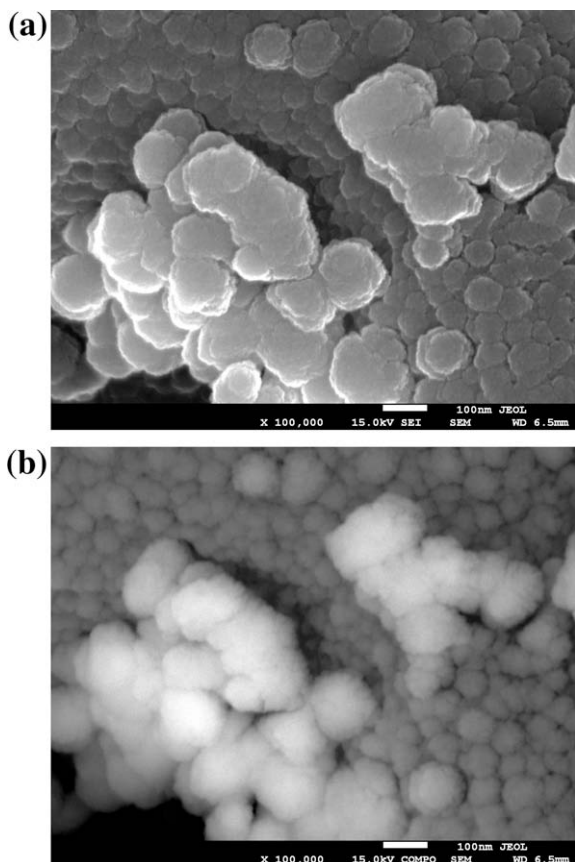


Fig. 7. SEM micrograph of NaBH_4 treated 2%Ru/FCN obtained with SEI (a) and COMPO (b) detection modes (magnification 100,000).

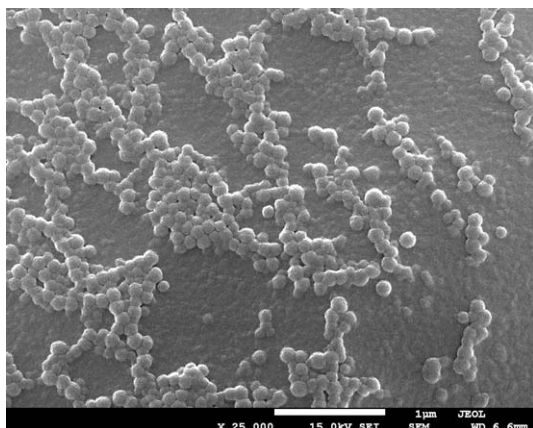


Fig. 8. SEM micrograph of parent FCN.

The XPS spectra of as-prepared 4%Ru/FCN composite showed two ruthenium states characterized by Ru $3d_{5/2}$ energy of 281.31 eV and 282.43 eV ($3p_{3/2}$ energy of 462.95 eV and 467.97 eV, respectively) (Table 3). The first Ru $3d_{5/2}$ energy of 281.31 eV ($3p_{3/2}$, 462.95 eV) is very similar to the energy of ruthenium state in starting reagent, RuCl_3 complex having the Cl ions as the ligands [37]. The appearance of the second ruthenium state with higher binding energy of 282.43 ($3p_{3/2}$, 465.97 eV) indicates the presence of a new type of Ru^{3+} ions surrounded most probably by N and O – containing ligands [37]. The binding energy observed for this component is similar to that reported for potassium dichloro (4,4'-(1,2-propylenediimino)-bis(4-phenyl-butan-2-ona-

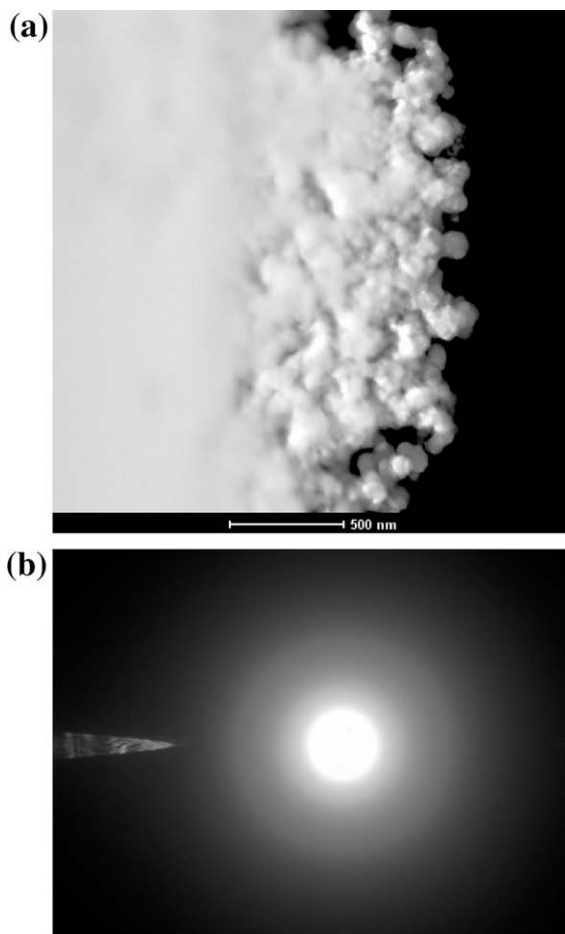


Fig. 9. STEM micrograph of NaBH_4 treated 2%Ru/FCN (a) and its diffraction pattern (b).

Table 3
Binding energies (BE) and contributions (%) of individual Ru^{3+} peak components.

Sample	Ru $3p_{3/2}$		Ru $3d_{5/2}$	
	BE (eV)	Contributions (%)	BE (eV)	Contributions (%)
$\text{RuCl}_3 \cdot x\text{H}_2\text{O}$	463.00	100	281.80	100
As-prepared 4%Ru/FCN	462.95	79.4	281.31	79.6
	465.97	20.6	282.43	20.4
NaBH_4 treated 4%Ru/FCN	463.16	66.3	281.33	66.8
	465.92	33.7	282.41	33.2

to))ruthenate(III) complex, $\text{K}[\text{Ru}(\text{CH}_3\text{C}(\text{O})\text{CH}(\text{C}_6\text{H}_5)\text{NCH}_2\text{CH}(\text{CH}_3)\text{N}=\text{C}(\text{C}_6\text{H}_5)\text{C}(\text{H})\text{C}(\text{O})\text{CH}_3)\text{Cl}_2]$, in which Ru is coordinated to N,O-containing ligands [38].

Hence, results obtained by the XPS technique are consistent with the FT-IR spectra showing the participation of functional groups of FCN polymer in the bonding of Ru-species. It should be stressed that the obtained XPS data are not quite representative for the whole analyzed composite, because of high inhomogeneity of Ru and Cl in individual composite beads (see Table 1). Therefore, XPS data may be considered as indicative of two types of Ru^{3+} states, whereas in view of EDS results (Tables 1 and 2) the contribution of such states may vary in different places of polymer beads.

In the XPS spectrum of NaBH_4 treated 4%Ru/FCN composite the same two states of Ru-species were observed (see Table 3). How-

ever the contribution of Ru-state of lower binding energy originating from Ru³⁺-Cl decreased (from 79.4% to 66.3%) at the expense of Ru-state with higher binding energy (465.92 eV) ascribed to Ru³⁺ ions surrounded by N and/or O containing ligands. In fact, the content of Cl in reduced composites decreased (Table 1). This suggests some type of “reorganization” in the nearest environment of Ru³⁺ ions upon the NaBH₄ treatment, which acted as the reducing agent mostly towards the Ru–Cl species. Noteworthy, in the NaBH₄ treated 4%Ru/FCN composite surface no peaks assignable to metallic Ru (Ru 3d_{5/2}, 280.6 eV, 3p_{3/2}, 462 eV) [37] can be seen. It has to be born in mind that XPS is a surface sensitive technique, and it provides information only from the most external surface layer of the solid (ca. few nanometers). The result shows that surface ruthenium species probed by the XPS technique become reoxidized after exposure of the catalyst to air.

3.5. Swelling measurements

The FCN resin consists mostly of non-polar constituents such as styrene (ca. 77 mol%) and smaller number of polar groups such as carbonyl and N-groups. This composition makes FCN resin relatively hydrophobic, and THF (dielectric constant, $\epsilon = 7$) was found to be the solvent resulting in the best expansion of FCN beads [14]. Therefore, swelling ability of pure FCN and as-prepared Ru/FCN composites was examined in THF solvent and the obtained data are collected in Table 4. These data show that the parent FCN polymer swells very well in THF and the volume of its beads increases 4.8-times. After incorporation of Ru-species the expansion of polymer mass in THF remarkably decreases, being only 2.4–3.2. No clear trend indicating the influence of the content of incorporated ruthenium upon the swelling ability was observed. The reduced swelling ability of Ru/FCN composites indicates that the structure of ruthenium–polymer composite becomes more rigid. This can be related to the formation of a “more crosslinked” polymer network. As demonstrated by the physical–chemical characterization, ruthenium–polymer complex is formed with the participation of functional groups of FCN polymer. Apparently, such a complex acts as an additional crosslinker. A similar phenomenon was observed in the case of Ru(III)-complexes coordinated by glycine modified chloromethylated styrene–divinyl benzene co-polymer [20].

It should be noted that FCN polymer (and Ru/FCN composites) do not swell in isooctane and water, i.e. the solvents used in present catalytic hydrogenation experiments.

3.6. DSC studies

DSC experiments were performed for FCN resin, as-prepared and NaBH₄ treated Ru/FCN composites and the values of the glass transition temperatures (T_g) are presented in Table 5. These data show that the insertion of Ru³⁺-species leads to T_g rise from 130 °C for parent FCN up to ca. 141 °C for as-prepared Ru/FCN composites. No influence of the ruthenium loading in FCN polymer on the value of T_g is noticed. An increase of glass transition temperature indicates more rigid polymer backbone, which may result from more crosslinked polymer. Thus, the observed increase of T_g

Table 4
Swelling ability (V_s/V_o) of pure FCN polymer and as-prepared Ru/FCN composites in THF solvent.

Sample	V_s/V_o
Pure FCN	4.8
1%Ru/FCN	2.6
2%Ru/FCN	3.2
4%Ru/FCN	2.4

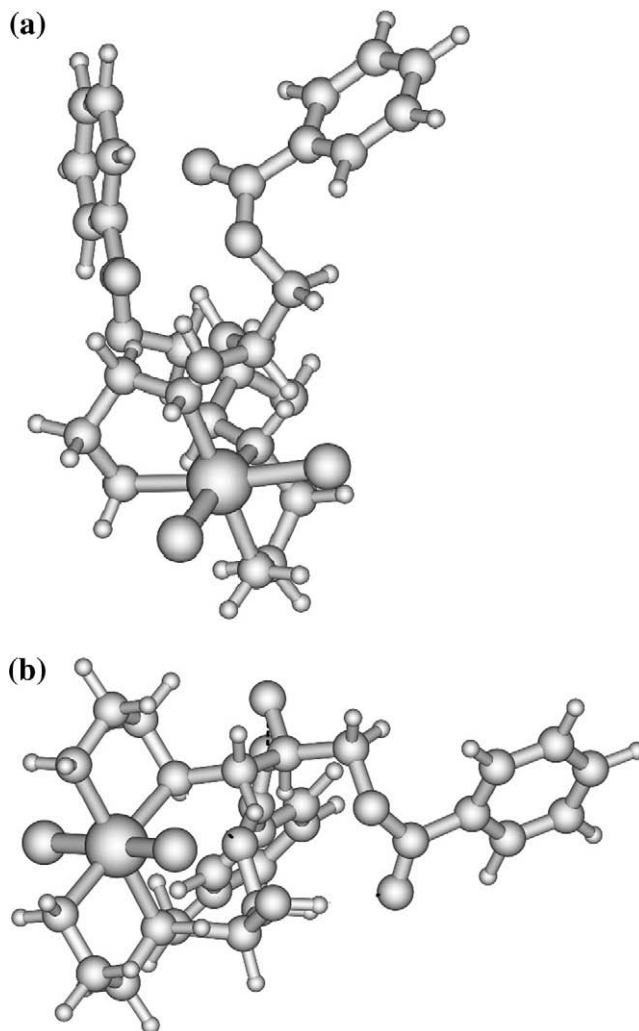
Table 5

The values of glass transition temperature T_g (°C) determined for parent FCN, as-prepared and NaBH₄ treated Ru/FCN composites.

Sample	T_g (°C)
FCN	130
As-prepared 1 wt.%Ru/FCN	141
NaBH ₄ treated 1 wt.%Ru/FCN	150
As-prepared 2 wt.%Ru/FCN	147
NaBH ₄ treated 2 wt.%Ru/FCN	151
As-prepared 4 wt.%Ru/FCN	140
NaBH ₄ treated 4 wt.%Ru/FCN	160

quite well confirms additional crosslinking of FCN polymer by Ru complex. The treatment of as-prepared Ru-composites by NaBH₄ results in further increase of T_g evidencing even higher crosslinking of polymer due to greater participation of functional groups of FCN polymer in coordination of Ru³⁺ ions, observed also by the XPS analysis. Thus, similarly to the observation of other authors, participation of polymer in the Ru-complexes has a direct effect on the properties of Ru-composites such as swelling ability of polymer mass and the temperature of glass transition [1,8].

In conclusions, all employed methods (FT-IR, XPS, XRD, EDS, SEM and STEM) show that ruthenium is indeed bound chemically



Scheme 3. Theoretical structures of “cis” (a) and “trans” (b) isomers of Ru/FCN composite.

to the FCN polymer. The anchoring of Ru-complexes occurs with participation of functional groups of the FCN resin, and involves particularly the N-groups.

Reacting of RuCl_3 with functional groups having glycine functionalized styrene-DVB polymer resulted in Ru-complexes in which four coordination positions were occupied by functional groups (N, C=O) whereas parent Cl-ligands located in two axial positions [20]. Similar coordination sphere was postulated in poly(styrene-DVB)-supported amino acid-Ru(III) complexes having two Cl-ligands in axial positions whereas four coordination positions were occupied by two chelating N,O ligands [33]. The presence of the two types of N-groups e.g. $-\text{NH}$ and $-\text{NH}_2$ in the structure of FCN polymer (Scheme 1) was confirmed in previously published data [14]. Thus, in the view of strong coordination ability of Ru(III) ions and the above described literature reports [20,33] two hypothetical structures (cis and trans isomers) of Ru-complexes formed with functional groups ($-\text{NH}_2$ and $-\text{NH}$) of polymer were taken into account (see Scheme 3 and Table 6). In the proposed structures, the presence of two Cl ions is assumed based on the EDS analysis. In all as-prepared samples Cl/Ru atomic ratio did not exceeded two (see Tables 1 and 2). Moreover, the Ru-species identified by Patel et al. [20] and Valodkar [33] in which Ru was coordinated to $-\text{NH}$ ligands also contained two Cl ions in axial positions. The comparison of total energies of the two complexes indicates the “trans” isomer as predominant in the real system (its total energy is lower than total energy of “cis” species by 27 kJ/mol). In “trans” isomer, the central ruthenium atom is equatorially coordinated to nitrogen atoms originated from polymer functional groups. The Ru–N bonds are slightly longer when formed with the participation of nitrogen from terminal $-\text{NH}_2$ group than with nitrogen from internal $-\text{NH}$ group. Two chains are practically equidistant from ruthenium and in this sense they may be considered as being equivalent. The relatively small difference in Ru–Cl bond lengths (0.009 Å) results from the steric hin-

drances exerted on the center of the complex by bulky polymer chains. In “cis” isomer, on contrary, there are larger discrepancies between ruthenium–nitrogen bond lengths from two chelating polymer functional groups. It is seen that nitrogen atoms from one functional group bind at the same distance (approx. 2.16 Å) to the central metal, whereas these from the second one form two non-equivalent bonds: shorter (with $-\text{NH}_2$ group) and longer (with $-\text{NH}$). Here, the difference between two Ru–Cl bond lengths is large than in “trans” isomer (it amounts to 0.019 Å), but the reason for this seems to be the same. Thus, calculated energies indicate that the formation of “trans” isomer with two axial Cl ions is preferred, similarly to what was reported by Patel et al. [20] and Valodkar et al. [33]. The participation of C–OH groups of FCN polymer seems to be less probable because no changes in the FT-IR spectral region of hydrogen bonds vibration were observed after immobilization of ruthenium complexes. Moreover, it cannot be excluded that octahedral symmetry of Ru^{3+} complexes together with the chelating action of polymer groups forces the occurrence of “disordering” of polymer framework with consequent remarkable changes in morphology of Ru-containing polymer beads.

3.7. Hydrogenation of acetophenone

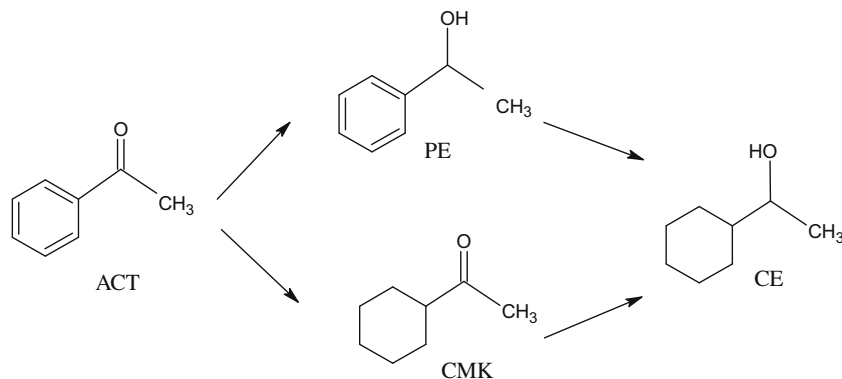
The catalytic hydrogenation of acetophenone (ACT), used here as a test reaction, is an important process of industrial relevance. The intermediates and/or products of this reaction e.g. 1-phenylethanol (PE), cyclohexyl methyl ketone (CMK), 1-cyclohexylethanol (CE) are widely used in pharmaceutical, cosmetic, food, agrochemical, and chemical industries. The most desired 1-phenylethanol, formed by the hydrogenation of carbonyl group of acetophenone, found an application as a fragrance or an intermediate in synthesis of various pharmaceuticals. Since many products are formed in the course of ACT hydrogenation, achieving high selectivity toward 1-phenylethanol, being a desired product is a complicated issue.

In the present work the results of preliminary catalytic experiments are shown. Further catalytic work is in progress in order to shed more light on the catalytic behavior of Ru/FCN composites. Here, catalytic efficiency of 2%Ru/FCN composite is compared with that of 2%Ru/ Al_2O_3 catalyst. In experiments Ru/FCN catalyst reduced by NaBH_4 was used because no hydrogenation reaction of ACT was observed in the presence of as-received catalyst. The activity of both Ru/FCN and Ru/ Al_2O_3 catalysts in organic solvents such as ethanol, THF and isoctane was very low, practically no measurable under conditions used in present experiments. Therefore biphasic system composed of two solvents e.g. water and isoctane (1:1 V/V) was used, similarly to what was reported by

Table 6

Computed parameters of proposed “trans” and “cis” binding modes of ruthenium atom to polymer chain.

	“trans”	“cis”
Relative energy (kJ/mol)	0	27
Bond length (Å)		
Ru–Cl	2.366	2.356
Ru–Cl	2.357	2.337
Ru– NH_2	2.144	2.134
Ru–NH	2.170	2.219
Ru– NH_2	2.147	2.167
Ru–NH	2.168	2.169



Scheme 4. Hydrogenation of acetophenone.

Perosa et al. [39] for hydrogenation of ACT in the presence of Pt/C catalyst. The role of a biphasic solvent system is discussed in detail in a forthcoming paper [40]. Briefly, the enhanced activity and selectivity is interpreted as due chiefly to favourable modification of polar properties of the reaction participants (reactants, catalyst surface and solvents). The obtained data of catalytic experiments are summarized in Fig. 10. It can be seen that after ca. 400 min of reaction conversion of ACT attained about 70% (Fig. 10a) in the presence of both catalysts, although the “shape” of curves differed. An induction period is observed on 2%Ru/Al₂O₃ catalyst only. In the presence of both catalysts the dominant reaction was hydrogenation of C=O of ACT to give 1-phenylethanol (PE). The contribution of other reactions, such as hydrogenation of aromatic ring of ACT or PE yielding cyclohexyl methyl ketone (CMK) and cyclohexylethanol (CE), respectively, proceeded to a much lesser extent. Formation of ethylbenzene is marginal on ruthenium catalysts [21,22] and in fact no ethylbenzene was observed in the present catalytic

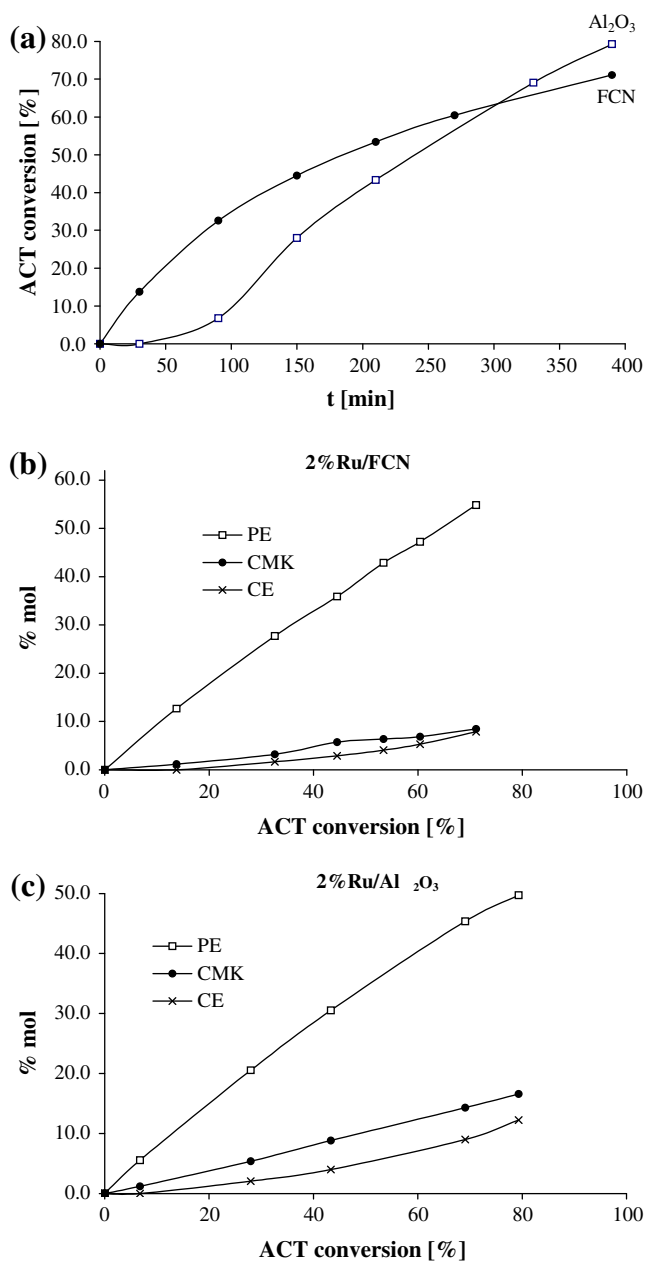


Fig. 10. Comparison of catalytic activity of 2%Ru/FCN with that of 2%Ru/Al₂O₃.

Table 7

The composition of reaction mixture at 50% ACT conversion and selectivity (S) to phenylethanol determined at 70% ACT conversion.

Catalyst	t (min) ^a	PE (mol%)	CMK (mol%)	CE (mol%)	S to PE (%)
2%Ru/FCN	188	40.3	6.3	3.4	77
2%Ru/Al ₂ O ₃	242	34.6	10.0	5.4	67

Reaction conditions: 20 cm³ of ACT solution in water–isooctane (1:1 V/V) initial ACT concentration of 0.137 mol/dm³, 0.2 g of catalyst, reaction temperature of 40 °C.

^a Time (min) required to reach 50% ACT conversion.

tests. It can be seen from Fig. 10b and c that the contribution of side reactions involving hydrogenation of aromatic ring was especially low in the presence of 2%Ru/FCN catalyst. As a consequence, at 50% ACT conversion, the dominating product in the reaction mixture was PE, a desirable product (Table 7). The selectivity to PE in final solution (ACT conversion ca. 70%) was calculated to be 77% and 67% (see Table 7) for 2%Ru/FCN and 2%Ru/Al₂O₃ catalysts, respectively. The relatively high selectivity towards phenylethanol (PE) shows preferential activity of polymer-supported Ru catalysts under present hydrogenation conditions towards the conversion of acetophenone via hydrogenation of carbonyl groups, whereas the hydrogenation of aromatic ring is strongly suppressed. It should be also noted that the obtained selectivity to PE is higher than that reported for Ru/TiO₂ or Ru/SiO₂ catalysts (50% and 18%, respectively) [24]. Therefore, more catalytic experiments are needed to clarify such highly efficient catalytic system and the studies are under progress.

4. Conclusions

By reacting of RuCl₃ with swollen matrix of FCN polymer containing diamine (–NH, –NH₂ functional groups) a series of Ru/FCN composites with various Ru loading (1%, 2%, and 4%) was prepared. Physico-chemical characterization proved the participation of polymer functional groups in the coordination of Ru(III). The coordination sphere around Ru trapped within the polymer matrix contained both Cl- and N-ligands in various proportions depending on ruthenium loading in polymer. Taking into account the chelating character of N-ligands a hypothetical structure of octahedral Ru(III) complex coordinated to FCN polymer was proposed. One of these composites, 2%Ru/FCN when reduced by NaBH₄ exhibited catalytic activity in liquid phase hydrogenation of acetophenone. Higher selectivity in the presence of FCN supported Ru as compared to 2%Ru/Al₂O₃ catalyst toward 1-phenylethanol was observed.

Acknowledgements

D.D. acknowledges the financial support from the POL-POST DOC II (Project D037/H03/2006) and Grant NN204 249034 (project 2490/B/H03/2008/34).

References

- [1] A.D. Pomogailo, V.N. Kestelman, *Metallopolymer Nanocomposites*, Springer-Verlag, Berlin, 2005.
- [2] A. Biffis, B. Corain, Z. Cvengrosová, M. Hronec, K. Jerabek, M. Kralik, *Appl. Catal. A: General* 124 (1995) 355.
- [3] R. Fisera, M. Kralik, J. Annus, V. Kratky, M. Zecca, M. Hronec, *Collect. Czech. Chem. Commun.* 63 (1987) 1763.
- [4] M. Kralik, R. Fisera, M. Zecca, A.A. D'Archivio, L. Galantini, K. Jerabek, B. Corain, *Collect. Czech. Chem. Commun.* 63 (1998) 1074.
- [5] A.K. Zharmagambetova, V.A. Golodov, Yu. P. Saltykov, *J. Mol. Catal.* 55 (1989) 406.
- [6] A.K. Zharmagambetova, E.E. Ergozhin, Y.L. Sheludyakov, S.G. Mukhamedzhanova, I.A. Kurmanbayeva, B.A. Selenova, B.A. Utkelov, *J. Mol. Catal. A: Chem.* 177 (2001) 165.

- [7] P. Centomo, M. Zecca, S. Lora, G. Vitulli, A.M. Caporusso, M.L. Tropeano, C. Milone, S. Galvagno, B. Corain, *J. Catal.* 229 (2005) 283.
- [8] Z.M. Michalska, K. Strzelec, *J. Mol. Catal. A: Chem.* 177 (2001) 89.
- [9] P. Hodge, *Chem. Soc. Rev.* 26 (1997) 417.
- [10] B. Corain, M. Zecca, K. Jerabek, *J. Mol. Catal. A: Chem.* 177 (2001) 3.
- [11] A. Biffis, B. Corain, Z. Cvengrosova, M. Hronec, K. Jerabek, M. Kralik, *Appl. Catal. A: General* 142 (1996) 327.
- [12] A. Drelinkiewicz, A. Waksmundzka, W. Makowski, J.W. Sobczak, A. Krol, A. Zieba, *Catal. Lett.* 94 (2004) 143.
- [13] A. Drelinkiewicz, A. Zieba, A. Krol, J.W. Sobczak, M. Grzywa, *Polish J. Chem.* 82 (2004) 1717.
- [14] A. Drelinkiewicz, A. Knapik, W. Stanuch, J. Sobczak, A. Bukowska, W. Bukowski, *React. Funct. Polym.* 68 (2008) 1650.
- [15] A. Drelinkiewicz, A. Knapik, W. Waksmundzka-Gora, A. Bukowska, W. Bukowski, J. Noworol, *React. Funct. Polym.* 68 (2008) 1059.
- [16] A. Knapik, A. Drelinkiewicz, M. Szaleniec, W. Makowski, A. Waksmundzka-Gora, A. Bukowska, W. Bukowski, J. Noworol, *J. Mol. Catal. A: Chemical* 279 (2008) 47.
- [17] B. Corain, M. Kralik, *J. Mol. Catal. A: Chem.* 159 (2000) 153.
- [18] R.A. Sanchez-Delago, N. Machalaba, N. Ng-a-qui, *Catal. Commun.* 8 (2007) 2115.
- [19] M. Hronec, Z. Cvengrosova, M. Kralik, G. Palma, B. Corain, *J. Mol. Catal. A: Chem.* 105 (1996) 25.
- [20] D.R. Patel, M.K. Dalal, R.N. Ram, *J. Mol. Catal. A: Chem.* 109 (1996) 141.
- [21] P. Kluson, L. Cervený, *Appl. Catal. A: General* 128 (1995) 13.
- [22] P. Kluson, L. Cervený, *J. Mol. Catal. A: Chem.* 108 (1996) 107.
- [23] P. Maki-Arvela, J. Hajek, T. Salmi, D. Yu Murzin, *Appl. Catal. A: General* 292 (2005) 1.
- [24] A.A. Wismeijer, A.P.G. Kieboom, H. van Bekkum, *React. Kinet. Catal. Lett.* 29 (1985) 311.
- [25] A.D. Becke, *Phys. Rev. A* 38 (1988) 3098.
- [26] J.P. Perdew, *Phys. Rev. B* 33 (1986) 8822.
- [27] Turbomole V5.9, a development of University of Karlsruhe and Forschungszentrum Karlsruhe GmbH, 1989–2007, Turbomole GmbH, since 2007. <<http://www.turbomole.com>>.
- [28] T. Koga, H. Kobayashi, *J. Chem. Phys.* 82 (1985) 1437.
- [29] T. Helgaker, *Chem. Phys. Lett.* 182 (1991) 503.
- [30] M. Nurunnabi, K. Murata, K. Okabe, M. Inaba, I. Takhara, *Catal. Commun.* 8 (2007).
- [31] L. Ma, D. He, *Top. Catal.* 52 (2009) 834.
- [32] The International Centre for Diffraction Data. <<http://www.icdd.com>>.
- [33] V.B. Valodkar, G.L. Tembe, M. Ravinadranathan, H.S. Rama, *J. Mol. Catal. A: Chem.* 223 (2004) 31.
- [34] P. Forment, M.J. Genet, M. Devillers, *J. Electron. Spec. Relat. Phenomen.* 104 (1999) 119.
- [35] V. Mazziari, F. Coloma-Pacual, A. Arcoya, P.C. L'Argentiere, N.S. Figoli, *Appl. Surf. Sci.* 210 (2003) 222.
- [36] X. Yan, H. Liu, K.Y. Liew, *J. Mater. Chem.* 11 (2001) 3387.
- [37] US National Institute of Standards and Technology (NIST) XPS Database. <<http://srdata.nist.gov/xps>>.
- [38] M.M.T. Khan, S. Srivastava, *Polyhedron* 7 (1988) 1063.
- [39] A. Perosa, P. Tundo, M. Selva, *J. Mol. Catal. A: Chem.* 180 (2002) 169.
- [40] D. Duraczynska, A. Drelinkiewicz, E. Bielanska, E.M. Serwicka, L. Litynska-Dobrzynska, *J. Mol. Catal. A: Chem.*, submitted for publication.